Sedimentology (2003) doi: 10.1046/j.1365-3091.2003.00554.x

Breaching in fine sands and the generation of sustained turbidity currents in submarine canyons

DICK R. MASTBERGEN* and JAN H. VAN DEN BERG†
*Department of Marine and Coastal Management, Delft Hydraulics, PO Box 177, 2600MH Delft, The Netherlands
†Department of Physical Geography, Utrecht University, PO Box 80115, 3508TC Utrecht, The Netherlands (E-mail: r.vandenberg@geog.uu.nl)

ABSTRACT

Natural, moderately loosely packed sands can only erode from the surface of the bed after an increase in pore volume. Because of this shear dilatancy, negative pore pressures are generated in the bed. In cases of low permeability, these negative pressures are released relatively slowly, which retards the maximum rate of erosion. This effect is incorporated in a new, analytically derived, pick-up function that can explain the observation of gradual retrogressive failure of very steep subaqueous slopes, sometimes more than 5 m high, in fine non-cohesive sands. This process, termed 'breaching' in the field of sediment dredging, may produce large failures in sand bars or river banks. The analytical function that describes the breaching process in fine sand is incorporated in a one-dimensional, steady-state numerical model of turbidity currents describing the spatial development of flow. This model is applied to simulate a large 'flushing' event in Scripps Submarine Canyon, Pacific coast of California. Breach retrogradation and the successive evolution in time of the resulting turbidity current in the canyon are predicted in a sequence of discrete steps. Predicted velocities are compared with values measured during a flushing event. Implications for the interpretation of deep-water massive sands are discussed.

Keywords Breaching, massive sands, slope failure, submarine canyon, turbidity current.

INTRODUCTION

In fine sand, because of gravity-related shear deformation and resulting negative pore pressures, very steep, gradually retrograding slopes, up to vertical, can exist for some time. In the field of sediment dredging, the process of gradual retreat of such a steep slope or breach is termed 'breaching' (Van Kesteren *et al.*, 1992; Van Rhee & Bezuijen, 1998; Van den Berg *et al.*, 2002). Two types of breaches can be distinguished, initiated by a supercritical (I) or subcritical (II) flow. The first type is found in series of bedforms formed at high Froude numbers, termed cyclic steps by Parker (1996) and analysed by Winterwerp *et al.* (1992), that can be considered as an adaptation of chute-and-pool bedforms to conditions in fine sand and silt. Much larger type I breaches may also develop as a single step in the first stage of the bursting of an embankment (Visser, 1998; Coleman *et al.*, 2002). Type II breaches can be generated incidentally on steep, perhaps up to >5 m high, submerged slopes on bars or channel banks. In contrast to a liquefaction slope failure, a breach retrogrades slowly and may be active for a large number of hours, producing a quasi-steady turbidity current.

In dredging practice, the breaching process is applied in sand mining in deep sand pits with cutter and suction dredgers, where the required initial steep slope can be made by suction. In nature, a breach may be initiated by the scar of a small shear failure. According to Kneller & Branney (1995), thick, massive sand layers preserved in some turbidite successions are an indication of prolonged quasi-steady flow

conditions during their deposition. Such a flow may be compatible with the breach failure mechanism. The sedimentological importance of breaching as an alternative to the generally assumed liquefaction mode of failure in fine sands was stressed by Van den Berg *et al.* (2002).

The main objective of the present paper is to provide a quantitative analysis of the breaching process and the resulting density under flow. The mechanism of breaching is related to the generation of negative pore pressures that retard rapid erosion processes due to flow or, in the case of a steep slope, to gravity. Thus, breaching is in fact a special case of a more general mechanism of erosion retarded by negative pore pressure. The first aim of this paper is to show how these pressures influence the pick-up rate of non-cohesive particles for any slope angle of the bed between horizontal and vertical. Secondly, the paper will present evidence of breaching as a mechanism of slope failure in submarine canyons. A simulation of such an event will be presented, using a one-dimensional model of breach growth and sand suspension density flow. The computational results are compared with flow velocity measurements obtained near the bed of a submarine canyon during a mass failure event as reported by Inman *et al.* (1976). A possible breach origin for some deep-water massive sands is discussed briefly.

BREACH EROSION EXPRESSION: RETARDATION OF EROSION BY NEGATIVE PORE PRESSURE

In flows over a sand or gravel bed, the erosion rate can generally be described with a function based on the flow-induced bed shear stress and the properties of individual sand particles only (Van Rijn, 1984a, 1993). In dimensionless form, and according to Winterwerp *et al.* (1992), the erosion rate or erosion velocity, Φ:

$$\Phi = A(\theta - \theta_{cr})^m D_*^n \qquad (1)$$

for $\theta > \theta_{cr}$. $\Phi = 0$ in case that $\theta \leq \theta_{cr}$ with: Φ = dimensionless pick-up rate or erosion velocity ($\Phi \geq 0$), defined as:

$$\Phi = \frac{E}{\rho_s \sqrt{\Delta g D_{50}}} \qquad (2)$$

E = sediment pick-up rate perpendicular to the bed ($\mathrm{kgs^{-1}m^{-2}}$), $D_* = D_{50}\sqrt[3]{(\Delta g/\nu^2)}$ = dimensionless grainsize (Bonnefile) parameter, A = coefficient (about 0·018), m = shear stress power in erosion function ($m = 1{\cdot}5$), n = grain size power in erosion function (n = 0·3), Δ = relative density of particles $(\rho_s - \rho_w)/\rho_w$ (= 1·60 in case of quartz particles), ρ_w = density of sea water ($\mathrm{kgm^{-3}}$), ρ_s = density of particles ($\mathrm{kgm^{-3}}$), g = gravity acceleration ($\mathrm{ms^{-2}}$), D_{50} = median grainsize (m), ν = kinematic viscosity of the sea-water ($\mathrm{m^2s^{-1}}$), depending on temperature, θ_{cr} = critical Shields bed shear stress (value depending on grainsize) and θ = bed shear stress or particle mobility parameter (–), according to:

$$\theta = \frac{\tau_0}{\rho_w \Delta g D_{50}} = \frac{f_0}{8}\frac{\rho_m}{\rho_w}\frac{\bar{u}^2}{\Delta g D_{50}} = \frac{f_0}{8}(1 + \Delta\bar{c})\left(\frac{\bar{u}}{v_s}\right)^2 \qquad (3)$$

in which τ_0 = bed shear stress (Pa), $\bar{u}$ = flow velocity averged over flow layer thickness ($\mathrm{ms^{-1}}$), v_s = (by definition) Shields-velocity for sand grains: $v_s = \sqrt{\Delta g D_{50}}$ ($\mathrm{ms^{-1}}$), f_0 = Darcy-Weisbach friction coefficient of a sand bed (value depending on grain roughness and, at low shear values, ripples, following Van Rijn (1984a) (–), $\rho_m = \rho_w(1 + \Delta\bar{c})$ = density of sand-water suspension ($\mathrm{kgm^{-3}}$), $\bar{c}$ = sand volume concentration averged over flow layer thickness (dimensionless or volume percentage). The net sand bed erosion velocity perpendicular to the bed v_e (in $\mathrm{ms^{-1}}$) now can be written, using Eq. 2, as:

$$v_e = \frac{E - S\cos\alpha}{\rho_s(1 - n_0)} = \frac{\Phi}{1 - n_0} v_s - v_{sed}\cos\alpha \qquad (4)$$

with n_0 the undisturbed (*in situ*) volume porosity of the sand bed (–) and in which the sedimentation rate of the sand bed S (in $\mathrm{kgs^{-1}m^2}$) is modelled according to Winterwerp *et al.* (1992), taking into account the hindered-settling effect, as:

$$v_{sed} = \frac{S}{\rho_S(1 - n_0)} = \frac{W_0 c(1 - c)^4}{1 - n_0} \qquad (5)$$

with v_{sed} the sedimentation velocity (in $\mathrm{ms^{-1}}$) and W_0 = fall velocity of single sand particle ($\mathrm{ms^{-1}}$). Equilibrium flow occurs when the net erosion velocity equals 0 and no net bed variation occurs.

In the case of a sloping sand bed, the erosion rate is supported because of a reduction in the effective shear resistance of the grains in the bed. At a slope steeper than the natural angle-of-repose, φ, the downslope component of gravity is

larger than the shear resistance, and unlimited erosion would result, until a slope smaller than the angle-of-repose was retained, even without any flow velocity-induced shear stress. However, on account of the generation of porewater underpressures in the bed, due to dilatancy effects, grain stresses are still present and the erosion rate is retarded. The horizontal retrogradation velocity, v_{wal}, of a slope steeper than the angle-of-repose termed the *wall velocity* in dredging practice (Breusers, 1974), appears to be independent of the local flow conditions. The wall velocity only depends on the porosity and permeability properties of the bed together with the local bed slope angle, α (Meijer & Van Os, 1976). From a stability analysis of the surface of the sloping bed, the following expression for the wall velocity was derived (Van Kesteren *et al.*, 1992; Van Rhee & Bezuijen, 1998):

$$v_{wal} = \frac{(1-n_0)\Delta \frac{\sin(\varphi-\alpha)}{\sin\varphi}}{\Delta n/k_l} \tag{6}$$

in which Δn = porosity increase in the sand bed from undisturbed to loose conditions, defined as $\Delta n = \frac{n_l - n_0}{1-n_l}$, n_l = porosity of the loose sand bed and after dilation, and k_l = permeability of the loose sand bed (m s^{-1}). The permeability of the undisturbed sand bed, k_0, is, according to the formula of Kozeny–Carmen:

$$k_0 = \frac{gD_{15}^2}{160\nu}\frac{n_0^3}{(1-n_0)^2} \tag{7}$$

in which D_{15} = 15th percentile of the cumulative bed material grain-size distribution (m). In loose sand, the porosity, n_l, should be substituted, resulting in a somewhat higher permeability, k_l. The wall velocity increases with the bed slope angle, α, until a maximum value is reached at a vertical step. At the latter condition ($\alpha = 90°$), the given expression reduces to:

$$v_{wal} = \frac{(1-n_0)\Delta}{\Delta n/k_l}\cot(\varphi) \tag{8}$$

With common values for natural sands, namely n_0 = 40–41%, Δ = 1·60, $\varphi = 30°$ and n_l = 44%, the expression for the breach retrogression velocity equals $\approx$20–25*k_0.

Winterwerp *et al.* (1992) proposed the following expression for the retrogressive erosion of steep slopes in the morphology of cyclic steps with $0 < \alpha \leq \varphi$:

$$\Phi\left\{1 - \frac{\tan(\alpha)}{\tan(\varphi)}\right\} = A(\theta-\theta_{cr})^m D_*^n \tag{9}$$

In the present analysis the flow vector is defined parallel to the bed slope, and the tangent terms are replaced by sine functions. To account for the reduction in erosion velocity due to the development of negative pore pressure gradients, allowing steeper slopes than the angle-of-repose, the erosion rate parameter Φ is multiplied by a relative erosion velocity factor in an analogous way (with $(\theta - \theta_{cr}) \geq 0$):

$$\Phi\frac{\sin(\varphi-\alpha)}{\sin(\varphi)}\left(1 - \frac{v_e}{v_{wal}}\right) = A(\theta-\theta_{cr})^m D_*^n \tag{10}$$

This formula yields a general second-order equation for the erosion velocity, v_e, which can be applied to a wide range of flow velocities. To show the effect of the net erosion velocity and the slope angle, Eq. 10 is further analysed. Substituting the expression for the net erosion velocity (Eq. 4) and neglecting the sedimentation velocity results in:

$$\frac{v_e}{v_s}\left(1 - \frac{v_e}{v_{wal}}\right) = \frac{A(\theta-\theta_{cr})^m D_*^n}{(1-n_0)\frac{\sin(\varphi-\alpha)}{\sin(\varphi)}} \tag{11}$$

On a steep retrograding breach ($\alpha = 90°$) with no flow velocity at all ($\theta = 0$), Eq. 11 implies that the erosion velocity equals the wall velocity, which is true for relatively small breach heights (Breusers, 1974). However, on account of soil mechanical failure of sand slices near the very steep top of >1 m high breaches, the actual retrogression velocity may be larger (Van Rhee & Bezuijen, 1998). The sand will be fully suspended downslope, and a continuous turbidity flow develops. Because of the extra bed shear generated by the accelerating flow, the actual erosion velocity increases downslope and can be much larger than the wall velocity. For low flow velocities, relatively large grains or high bed permeability and mild slopes, the classical sediment transport regime holds (Eq. 1). For these conditions in Eq. 11, the term v_e/v_{wal} is <<1 and therefore can be neglected (= 0). The solution then reads:

$$v_e = \frac{A(\theta-\theta_{cr})^m D_*^n}{(1-n_0)\frac{\sin(\varphi-\alpha)}{\sin(\varphi)}} v_s \tag{12}$$

For high erosion rates or fine sand with relatively low permeability, dilatancy effects play a role.

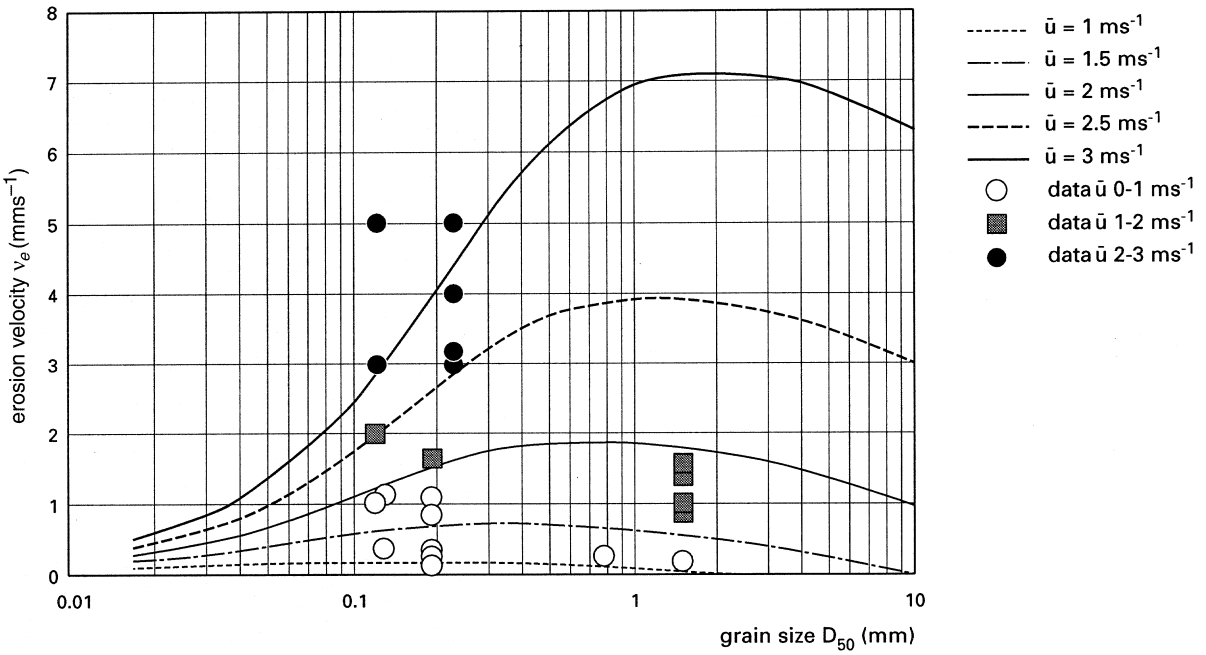

Fig. 1. Erosion velocity in sand as a function of grain size and flow velocity, with $A = 0{\cdot}018$, $\theta_{cr} = 0{\cdot}06$, a sea-water temperature of 15 °C and $f_0 = 0{\cdot}1$. Data obtained from Van Rijn (1984a, 1993): $D_{50} = 130$, 190, 790 and 1500 μm with $\bar{u} = 0{\cdot}5$–$1{\cdot}3$ m s^{-1}; and Winterwerp *et al.* (1992): $D_{50} = 120$ and 225 μm with $\bar{u} = 1$–$3{\cdot}5$ m s^{-1}.

Thus, in the limit, the term v_e/v_{wal} is >>1, and the value 1 between the brackets may be neglected, resulting in a square root solution:

$$v_e = \sqrt{\frac{-A(\theta - \theta_{cr})^m D_*^n}{(1 - n_0)\frac{\sin(\varphi - \alpha)}{\sin(\varphi)}} v_s v_{wal}} = \sqrt{\frac{A(\theta - \theta_{cr})^m D_*^n k_l \sqrt{\Delta^3 g D_{50}}}{\Delta n}} \qquad (13)$$

When the computed results, assuming $m = 1{\cdot}5$, $f_0 = 0{\cdot}1$ and $\theta_{cr} = 0{\cdot}06$, are plotted as erosion velocity vs. grain size (Fig. 1), a maximum appears in the curves of each selected depth-averaged flow velocity. With increasing flow velocity or bed slope, the maximum shifts to coarser grades. For large particles, depending on the flow velocity, in accordance with classical regime theory, the erosion rate decreases with increasing grain diameter. However, for fine sands, because of low permeability, the opposite is true, and erosion rate increases with increasing grain diameter. This effect is clearly confirmed by erosion tests in sand using high-pressure water jets, and by the experience in suction dredging that densely packed fine sand and silt are much harder to excavate than coarser sand (Van Kesteren *et al.*, 1992). The very high flow velocity related to these water jets, however, is beyond the scope of this paper. A sensitivity analysis of the breach erosion expression (Eq. 11) indicates that the typical optimum behaviour is defined by the value of the power m (enhanced for $m = 2$, reduced for $m = 1$) and the critical grain shear stress, θ_{cr} (enhanced for larger, reduced for smaller values than 0·06). Variations in water and sediment density and temperature (and hence water viscosity) result in a slight shift of the curves in Fig. 1. The influence of the actual porosity clearly demonstrates the effect of negative pore pressures; erosion strongly increases for n_0 approaching the critical value n_l and is undefined for larger values – the bed will thus not erode but collapse. Although Eq. 11 is sensitive for the value of the calibration parameter, A, the value cannot be defined independently from that of the friction coefficient because, in most experiments, only flow velocities have been measured without any direct shear stresses.

SLOPE FAILURES AT THE HEAD OF SUBMARINE CANYONS: THE EXAMPLE OF SCRIPPS SUBMARINE CANYON

Many submarine canyons that extend shorewards into the surf zone are presently serving as active

transport conduits for sand from the coastal zone to the shelf or even deeper waters (Dietz & Knebel, 1971; Inman *et al.*, 1976). Sand, transported by wave-induced currents in the nearshore zone, is temporarily trapped in the head of the canyon, until it is transported suddenly downcanyon. Although this type of submarine canyon is found along many coasts with steep narrow shelf zones, the present knowledge concerning their sediment dynamics is based on measurements and diver observations in Scripps Submarine Canyon. The present analysis adopts this canyon as an example and discusses possible causes of periodic flushing events that remove virtually all the sand fill in one or more branches of the canyon. A simulation is then presented of a flushing event in one of the branches, using a numerical model of breach retrogression and successive turbidity current.

Present explanations of sand removal and indications in favour of breaching

Scripps Submarine Canyon is one of the nine major submarine canyons that intersect the continental shelf off southern California. The canyon consists of a number of branches, eroded in Eocene sedimentary rocks. These branches join in a water depth of about 40 m and, in a shoreward direction, the head of each of these branches ends up in several tributaries. The tributaries may be up to 10 m wide, 20 m long and several meters deep and extend into the surf zone. The tributaries and the head of the branches are filled with sand most of the time, which may reach a thickness of 5 m (sometimes up to 10 m) and shows a depositional slope, which on average approximates the angle-of-repose (about 31°; Chamberlain, 1964). According to grain-size distributions presented by Shepard & Dill (1966), the sediment that is temporarily stored at the head of the canyon consists of well-sorted micaceous fine sands and coarse silts with a median ranging between 95 and 125 μm and up to a 10% admixture of organic detritus. The true form of the canyon head consists of narrow gorges with steep rock walls that are only apparent for 3–4 weeks at a time when mass removal of sediment exposes most of the rock surface (Dill, 1964a). A map showing the hydrography of the canyon is shown in Figure 2.

Scripps Submarine Canyon is part of a larger system and joins La Jolla submarine canyon at a depth of about 300 m, continuing seawards as a rock-walled valley to about 530 m depth, where a fan valley with levees cut into unconsolidated sediment is encountered (Shepard & Buffington, 1968). This fan finally terminates in the San Diego Trough, more than 1000 m below the sea level., By comparing successive hydrographic surveys, Chamberlain (1964) demonstrated that sudden large sand losses between 0·6 and $2{\cdot}3 \times 10^5$ m^3 occurred nine times in a period of 11 years. Such losses were often restricted to one branch, and the sand was transported downvalley by sediment gravity flows. According to Piper (1970), about 90% of the transported sediment is bypassing the fan and deposited in the San Diego Trough. The frequency at which a canyon branch is flushed varies and seems to be related to the rate of sand delivery from the coast to the branch. During periods of strong wave agitation, the sand deposit in the head of a canyon branch progrades rapidly into deeper water. In a few days, the face of this prograding sand bar may advance as much as 8 m. Chamberlain (1964) and Dill (1964b) suggested that, during this fast progradation, the face of the sand bar may become oversteepened and subject to sudden slumping, followed by the complete flushing of the bar sands, revealing the 'naked' narrow slot canyon, with boulders and terraces, as reported by divers. However, as slumping will be restricted to the bar face, such a failure alone cannot account for the virtually complete disappearance of the sand body. It has been proposed that the main failure mechanism of the complete sand bar was liquefaction (Shepard, 1951), although comparison of data on flushing events did not show any correlation with the occurrence of earthquakes (Chamberlain, 1960). Also, several experiments using explosives to induce liquefaction artificially have failed (Inman *et al.*, 1976). As a sand deposit is susceptible to either dilation or contraction, the exclusion of liquefaction implies a dilative behaviour of the sand upon shear deformation, which strongly supports breaching as the main failure mechanism. The steep scars left by small shear failures, as reported by divers (Dill, 1964a), might very well provide the starting point for an active retrograding breach with increasing height.

Fukushima *et al.* (1985) argued that ignitive turbidity currents might be responsible for the periodic flushing of large volumes of sand from the head of Scripps Submarine Canyon. Inman *et al.* (1976) reported that, during periods of high wave agitation, downchannel currents as strong as 0·5 m s^{-1} are generated. Based on a thorough theoretical analysis, Fukushima *et al.* (1985) demonstrated that this flow, combined with

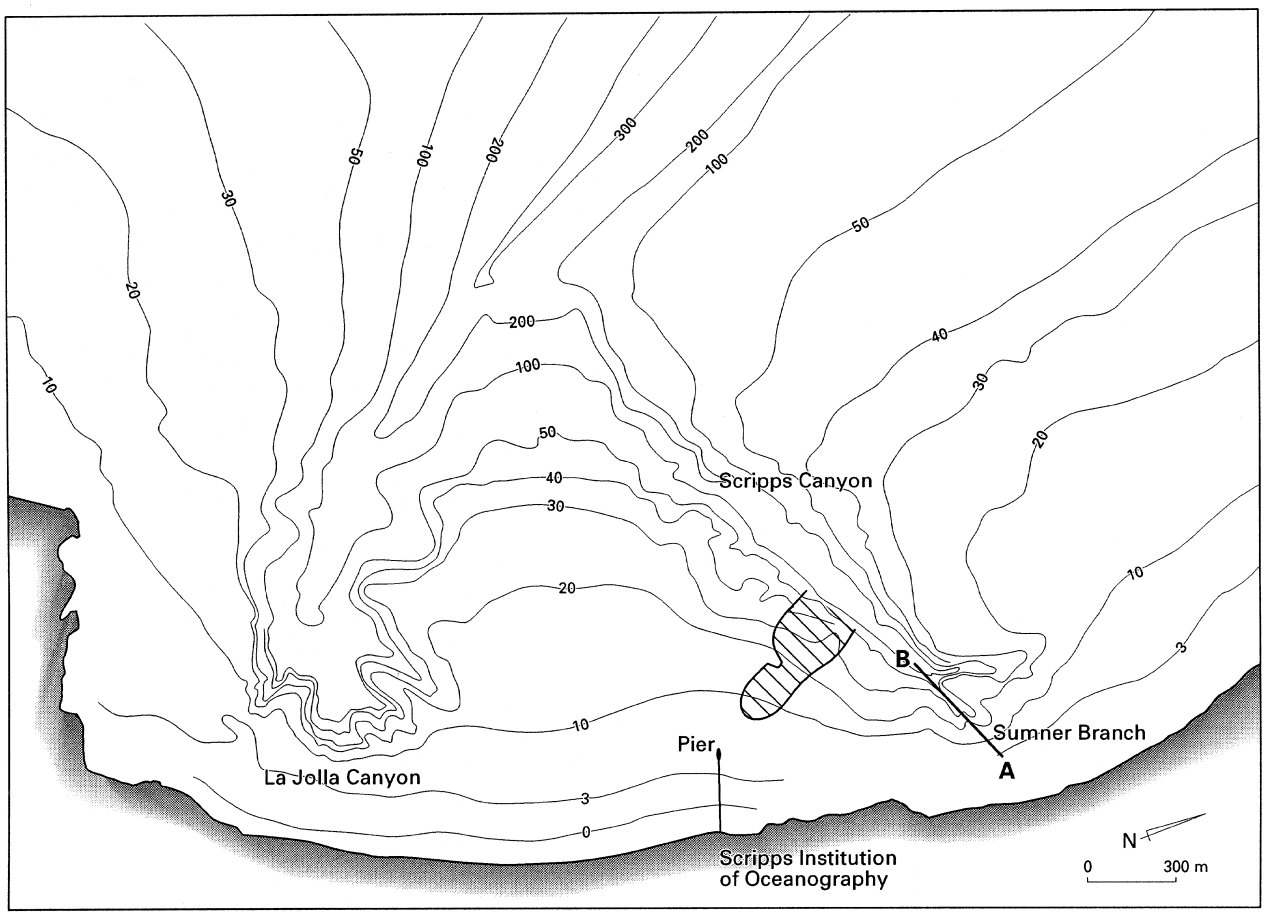

Fig. 2. Hydrography of La Jolla and Scripps Submarine Canyons. A–B denotes thalweg of Sumner Branch (shown in Fig. 4); cross-hatched area is location of 1975 'flushing' event (Marshall, 1978). Contours in metres below mean low water at spring tide.

calculated estimates of suspended sediment concentration and flow layer thickness, might ignite, i.e. accelerate and erode its bed as it flows down the canyon. As erosion of the bed continues until this supply is depleted, this theory provides an explanation of the complete disappearance of sand at the bottom of the canyon after a flushing event. It can also explain the occurrence of strong sustained currents in the canyon during storms, as reported by Shepard & Marshall (1978) and Inman *et al.* (1976). However, the theory of ignitive turbidity currents fails to give a full explanation of the flushing events in several respects. First, the postulation that strong wave agitation generates turbidity currents that erode the sand fill of the canyon is opposed by observations that such wave conditions promote the accretion of the sand bar in the head of the canyon. Secondly, if erosive currents are generated by strong wave agitation, it is difficult to reconcile why this only occasionally results in the removal of a sand fill and, if it does, why it generally does not affect all branches simultaneously (Dill, 1964b). The fills of two branches of the canyon were reported to have been flushed only once in the past century (Shepard, 1951; Chamberlain, 1964; Marshall, 1978). Thirdly, the theory of Fukushima *et al.* (1985) implies that ignitive turbidity currents should last as long as strong wave agitation is present and the source of sand is not depleted. At the head of the canyon, the velocity is of the order of 0·5 m s^{-1} (Inman *et al.*, 1976; Fukushima *et al.*, 1985), and the erosive capacity of the turbidity current is therefore small. Thus, in order to remove a sand fill completely, which is generally the case, conditions of strong wave agitation should last for an unreasonably long period of time. These objections should not lead to the conclusion that the theory of ignitive turbidity currents as the cause of the flushing of canyon heads must be rejected completely. The present paper contends that such currents may play an important role, but the source of the density flow should be considered

in conjunction with breaching instead of erosion by storm waves. Ignitive turbidity currents may possibly result in steepening of the bar face, and thus create the prerequisite conditions for initiation of an active breach. As breaching retrogrades into the bar face, it supports the strength of the turbidity current and increases its erosive capacity. Therefore, it is hypothesized that flushing events are the combined result of both processes. Although ignitive turbidity currents can explain a steepening of the bed slope and may help to sustain the breaching process, the initiation of breaching is most likely to be linked to the collapse of steep bar sections by a shear failure. Such slope instability may be favoured by rapid bar growth, for instance as a result of sand transport by storm-induced currents.

A breach-generated model of turbidity currents

Depending on the availability and properties of sand at the bed and the local bed slope, a breach-generated density flow may accelerate, creating an ignitive steady turbidity current *sensu* Parker (1982) and then either become unstable and dilute or decelerate and extinguish. The thickness of the density flow increases downslope as a result of entrainment of sea water at its upper boundary. Eventually, a quasi-steady flow will be maintained over a long distance and even over very flat slopes, before the sand particles settle and the flow dies out. In the past two decades, a number of mathematical models of turbidity currents have been developed, most of which are steady and one-dimensional depth-averaged (Parker *et al.*, 1986; Mulder *et al.*, 1998), although recently two-dimensional models are available (Felix, 2001), and fully three-dimensional models with erosion and deposition have been presented and successfully applied (De Cesare *et al.*, 2001). As Scripps Submarine Canyon is a more or less linear feature, a one-dimensional model should be able to represent satisfactorily the main characteristics of a turbidity current flowing through it. In the present analysis, a non-uniform, quasi-steady, two-layer, depth-averaged model is applied, including the breach erosion expression (Eq. 11). This model was originally developed to simulate the interaction of flow and bedforms in free surface flows in the case of cyclic steps at sites of sand deposition (Mastbergen, 1989; Winterwerp *et al.*, 1992). The model is derived from the basic momentum and continuity equations, taking into account the effects of high sediment concentrations, sedimentation and erosion processes and density effects, and is extended here to subaqueous sedimentary density flows. The two-layer schematization of the model is shown in Fig. 3. Although the flow slowly retrogrades, and net erosion takes place at the upper part, a quasi-steady flow schematization is allowed. The model has been calibrated among others with breaching experiments in a 2·5 m

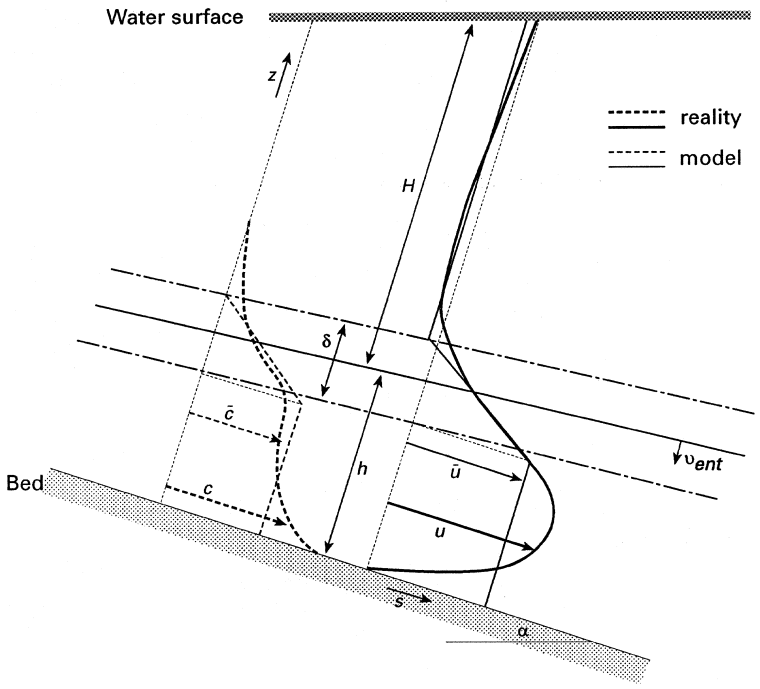

Fig. 3. Two-layer model schematization of flow velocity and sand concentration distribution.

deep flume with fine and medium fine sands (Van Rhee & Bezuijen, 1998). However, so far, no detailed data are available for accurate calibration of all parameters for field conditions.

In the present paper, the model is used to simulate breach-generated turbidity currents in Scripps Submarine Canyon. The model is based on a set of three equations:

(1) the momentum equation of the sand–water mixture flow sublayer under water, defined along slope direction s and slope angle α with the horizontal plane:

$$\rho_m \varepsilon g \cos\alpha h\left(\frac{dh}{ds} - \sin\alpha\right) + \frac{1}{2} g \cos\alpha h^2 \frac{d\rho_m}{ds} + \frac{d(\rho_m q u)}{ds} + (\tau_0 + \tau_i) = 0 \quad (14)$$

(2) the continuity of water:

$$\frac{d}{ds}[q(1-\bar{c})] = n_0 v_e + v_{ent} \quad (15)$$

and (3) the continuity of sediment:

$$\frac{d}{ds}[q\bar{c}](1-n_0)v_e \quad (16)$$

with the friction shear stress at the bed:

$$\tau_0 = \frac{f_0}{8}\rho_m \bar{u}|\bar{u}| \quad (17)$$

and in the internal boundary layer, between the density flow sublayer and ambient sea-water upper layer:

$$\tau_i = \frac{f_i}{8}\rho_m \bar{u}|\bar{u}| \quad (18)$$

The relative density difference of the suspension flow with the ambient sea water is defined as:

$$\varepsilon = \frac{\rho_m - \rho_w}{\rho_m} = \frac{\Delta c}{1 + \Delta c} \quad (19)$$

in which q = specific discharge = $\bar{u}h$ (m^2 s^{-1}), h = flow thickness (m), f_i = friction coefficient in the internal boundary layer, s = downstream distance along the bed (m) and τ_i = shear stress in the internal boundary layer (Pa).

The analysis of Ashida & Egashira (1975) suggests the approximation $f_i = 0{\cdot}33 f_o$. The thickness of the turbidity flow increases downstream because of entrainment of sea water at the upper boundary of the density flow and at the head of the flow. The dimensionless rate of water entrainment, E_w, is defined as:

$$E_w = \frac{v_{ent}}{u} \quad (20)$$

where v_{ent} = rate of water entrainment (m s^{-1}).

Since Lofquist (1960) determined experimentally that entrainment is inversely proportional to the Richardson number, various researchers have derived expressions for the case of turbidity currents (e.g. Parker *et al.*, 1987). In the present model, the equation proposed by Ashida & Egashira (1975) is adopted:

$$E_w = \frac{0{\cdot}0015}{Ri} \quad (21)$$

with the gradient Richardson number, Ri, defined as (Turner, 1973):

$$Ri = \frac{g}{\rho}\frac{\partial\rho/\partial z}{(\partial u/\partial z)^2} \quad (22)$$

in which ρ = density of sediment mixture flow at height z above the bottom (kg m^{-3}) and u = flow velocity at height z above the bottom (m s^{-1}).

The overall Richardson number Ri^* can be derived from the gradient Richardson number in the case of the present two-layer flow schematization. Assuming a linear concentration and velocity gradient in the intermediate layer with a thickness δ (see Fig. 3), the average density, $\rho = \rho_m$, flow velocity $\bar{u}$, flow depth h of the suspension flow sublayer and a flow velocity $\bar{u} = 0$ and density $\rho = \rho_w$ in the ambient water upper layer, substitution results in a simple expression for the overall Richardson number,

$$Ri^* = \frac{g}{\rho_w}\frac{\frac{\rho_m - \rho_w}{\delta}}{\left(\frac{\bar{u}}{\delta}\right)^2} = \frac{\varepsilon g h}{\bar{u}^2}\frac{\delta}{h} = Fr_i^{-2}\frac{\delta}{h} \quad (23)$$

with Fr_i = internal Froude number defined as:

$$Fr_i = \frac{\bar{u}}{\sqrt{\varepsilon g h}} \quad (24)$$

For density flow stability reasons (Kelvin–Helmholz instability), the Richardson number theoretically cannot become smaller than 0·25: at smaller values, rapidly growing billows develop at the interface of the density flow and the overlying fluid, which strongly enhance

entrainment (Thorpe, 1973). Moreover, the thickness of the sublayer cannot exceed half the intermediate layer, $h > 0{\cdot}5\delta$ (see Fig. 3). If the intermediate layer grew any further, the density flow would dilute completely. This results in the following stability criterion:

$$0{\cdot}25Fr_i^2 \leq \frac{\delta}{h} \leq 2 \qquad (25)$$

This criterion implies that the internal Froude number of the suspension flow cannot exceed a value of about 2·8. Strongly supercritical density flows, for instance on very steep slopes, will therefore dilute and disintegrate. On the other hand, subcritical flow is undefined if no downstream boundary condition is present, such as an obstruction or inflow. The range of internal Froude numbers (and successive slope, height, sand concentration and sand properties) that allows turbidity flows to be generated and persist is therefore quite narrow ($1 < Fr_i \leq 2{\cdot}8$). In the present two-layer schematization, the sublayer thickness of the flow h, including half the intermediate layer (see Fig. 3), is defined for continuity reasons as the distance from the bed for which:

$$\int_{z=0}^{h} u(z)dz = q \text{ resp. } \int_{z=h}^{H} u(z)dz = 0 \qquad (26)$$

with H = thickness of the upper layer (see Fig. 3). Substituting Ri^* in the expression for the entrainment and assuming a value for δ/h of 1 for the entrainment velocity results in:

$$v_{ent} = 0{\cdot}0015\bar{u}Fr_i^2 \qquad (27)$$

A comparable set of equations to describe the flow has been applied by Fukushima *et al.* (1985) to simulate ignitive turbidity currents in Scripps Submarine Canyon. The main difference here is the initiation mechanism. Fukushima *et al.* (1985) assumed agitation of edge waves as the source of the density flow which, as reasoned earlier, is probably incorrect. In the present analysis, the turbidity flow is generated by an active retrograding breach. This process is explicitly incorporated in the model by the breach sand erosion formula (Eq. 11), and the breaching commences in the steep scar of a shear failure. The scar slope is imposed as a boundary condition and, thus, the shear failure itself is not considered. In the model, multiple horizontal sand layers with various bed slopes and sand properties are considered (Fig. 4).

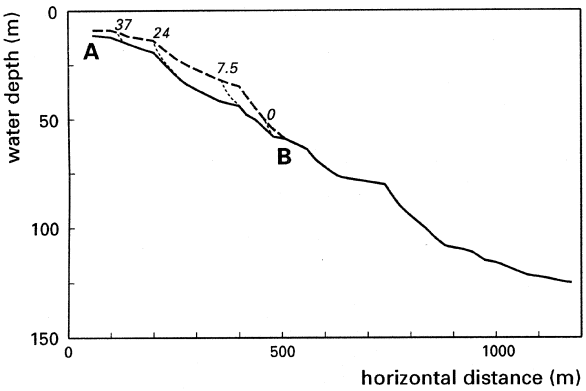

Fig. 4. Thalweg profile of Sumner Branch (see Fig. 2). Solid line is Eocene bedrock, and dashed line is top of sand fill. Dotted lines are stages of breach evolution after initiation of a breach at the toe of the sand fill. Time is indicated in hours after initiation of the breach.

The computations to solve the three coupled differential equations were carried out as follows. First, from Eqs 14, 15 and 16, the derivatives $d\bar{u}/ds$, dh/ds and $d\bar{c}/ds$ were solved analytically. Next, a simple forward explicit numerical scheme was used to solve the unknown $\bar{u}$, h and $\bar{c}$ as functions of s. For each step in the model, the slope angle, α, the height of the step and sand properties may vary. Besides flow velocity, depth and concentration, the net erosion or sedimentation velocity, flow rate, sand transport rate, Froude number and corresponding x *and* z co-ordinates were computed. The required upper boundary condition for flow values was introduced with a given initial sand transport rate, produced by an initial vertical breach (with a height of 1 m), retrogression velocity (1–2 mm s^{-1}), sand concentration (30%) and Froude number ($Fr_{i,0} = 2$). These values have only a local influence and do not affect flow velocity and concentration downslope in the canyon, as the flow adapts to local conditions very quickly.

Two computational model options can be used: (1) prediction of development of the equilibrium bed slope, given a retrogression velocity, as dictated for instance by the advancing suction head of a dredge by variation of the slope of each step; or (2) the autonomous natural process of flow and initial morphological changes resulting from active breaching on an existing slope. The latter option is used here to simulate a flushing event in Scripps Submarine Canyon starting from four different locations, representing four time steps in the continuous retrogression process. The governing

parameters defining flow velocity, erosion, sand concentration and sand transport in the model are, in order of importance: local bed slope, grain size, permeability, entrainment and friction. A sensitivity analysis with the model for the present bed topography shows that the influence of a 50% variation in the friction coefficient, f_0, which cannot be determined accurately, results in about 15% variation in flow velocity and 25% variation in flow depth of the turbidity current.

Application of the model to Scripps Submarine Canyon

Based on the topography of Scripps Submarine Canyon, computations have been made with the model in order to establish whether, and where, a breach-generated turbidity current is feasible and what flow properties will develop. The following field data input was used: sand with a median grain size, $D_{50} = 110$ μm, an *in situ* porosity of the sand bed of 38%, a permeability of $k_0 = 5{\cdot}9{*}10^{-5}$ m s^{-1}, a water temperature of 10 °C and a density of sea water, $\rho_w = 1020$ kg^{-3}. Figure 2 gives the bed topography used in the model and obtained from a map in Shepard & Dill (1966). The steepest part of the canyon, down to a depth of 110 m, represents Sumner Branch and is shown in more detail in Fig. 4.

The model simulation refers to the flushing event of 12–13 December 1959, described by Chamberlain (1960). Figure 4 shows the sand pocket, with a volume of $0{\cdot}1{*}10^6$ m^3 filling the head of the canyon before the event, as based on an isopach map provided by Chamberlain (1960). In the simulation here, it is assumed that breaching starts in the scar left by a small shear failure near the toe of the sand bar, where the steepest slope is found. The computations show whether or not a small initiating failure somewhere on the sand slope will result in a self-accelerating turbidity flow. If not, a small breach can still retrograde for some distance upslope, but no suspension flow will develop. It is assumed that, downvalley of the sand pocket, no sediment covered the Eocene rock bed.

Figure 5A–D displays the computational results, representing the flow development, initiated at the toe of the sand deposit. The sand released by the retrograding breach develops into an accelerating turbidity flow, eroding more and more sand from the bed, thus increasing the driving gravity force of the flow. However, when the bare canyon rock is encountered downcanyon from the initiation point, no more sand is incorporated in the turbidity current, and the flow will not accelerate any more but will still persist for a long distance (over 3 km). If sand were present over the full length of the slope, the flow would accelerate even more. From the point where bare

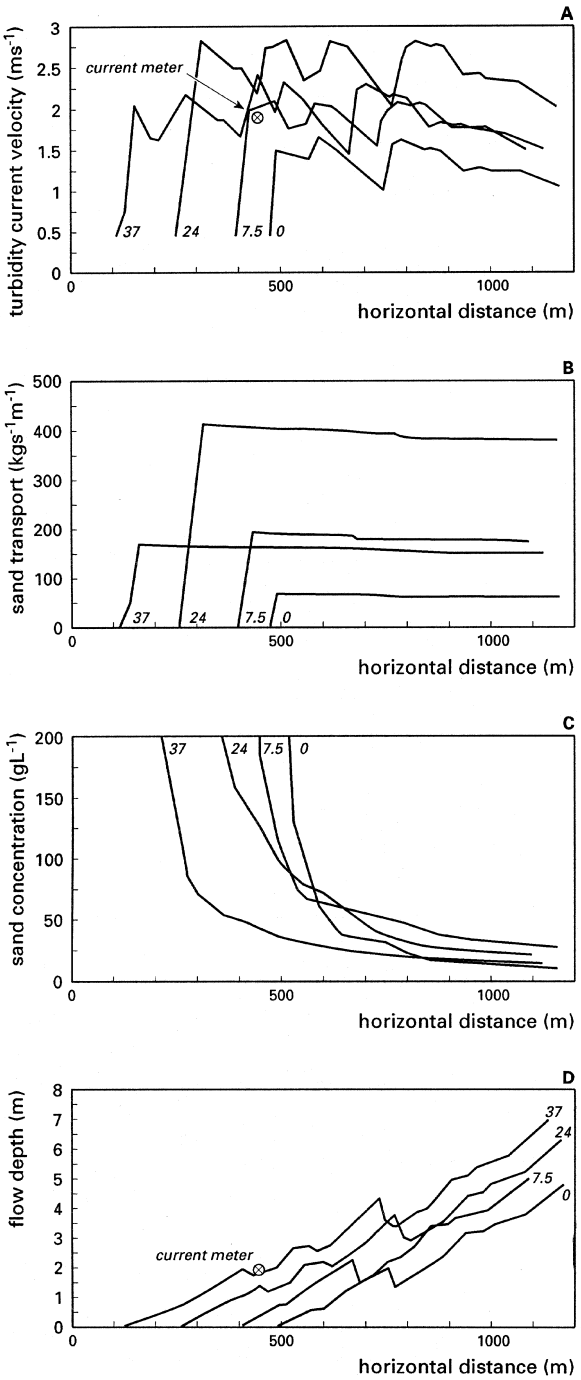

Fig. 5. Computed spatial and temporal evolution of the breach-generated turbidity flow in Scripps Submarine Canyon. (A) Flow velocity averaged over flow depth, *h*. (B) Depth-averaged sand transport. (C) Depth-averaged sand concentration. (D) Turbidity current flow depth, *h*. Time stages are indicated in Fig. 4.

rock is encountered, the sand transport rate remains constant, and any Lagrangian change in flow velocity is caused by slope only. Computations with the model that were extended to the lower parts of the canyon indicate that sediment deposition and flow decay, which will lead to a gradual disappearance of the turbidity flow, will not occur until gentle slopes of less than 1:20 are encountered. This is in accordance with the notion that most of the sand eroded from Scripps Submarine Canyon is deposited on the San Diego deep sea fan (Piper, 1970).

After its initiation on the steep slope, the breach will grow in height, and an increasingly larger area will contribute to the suspension current. As a result, sediment transport and flow velocity will increase gradually in time (Fig. 5).

After 7·5 h of retrogressive erosion, the breach height remains more or less stable. As a result, the suspension flow will not accelerate greatly any more, and the flow velocity is predicted to remain quasi-steady for many hours. The computations suggest that, in the canyon reach considered, the density flow is supercritical everywhere (internal Froude number 1·5–3). This implies that, if local flow obstructions are present, internal hydraulic jumps may occur, resulting in small, secondary retrogressive breaches. This also implies that, locally, on some very steep parts of the slope, the flow may accelerate to such a degree that it may become unstable and dilute ($Fr_i > 2{\cdot}8$). Both these high Froude number effects are not reproduced by the model. On more gentle parts of the sand bed in the canyon, no flow acceleration will take place. If breaching were initiated here, it would not result in an ignitive turbidity current. Breaching that is initiated downslope of the sand deposit and moves upslope, generating a sustained turbidity current, will continue until all the sand is flushed away from the canyon head. If the retrogressive velocity of the breach is assumed to be equal to the wall velocity, it is expected to abandon the narrow canyon 37 h after its initiation. The breach will then expand radially into the morphology of the gently sloping surf zone, while gradually losing height until the process finally ends.

Several decades ago, attempts were made to measure flow velocity near the canyon bed during a flushing event. Most of these attempts failed as the intensity of the flow destroyed the installation, except for one occasion. During a flushing event on of 24 November 1968, a current meter installed at 44 m depth, 2 m above the bottom of Sumner Branch, measured an almost steady flow velocity of 1·9 m s^{-1} over a period of 2·5 h, after which the sensor was lost (Inman *et al.*, 1976). This measured velocity is indicated on Fig. 5, and its flow strength and steadiness appear to be in good agreement with the computational results. However, the predicted thickness of the sublayer at the measuring point seems to be too thin. But small variations in entrainment rate or local canyon morphology may explain local variations in flow depth of the order of magnitude observed. Additionally, some discrepancy between computational results and measurements may be expected, as the simulated flushing event and the event from which the measurements were obtained are not the same. In the simulated case, the maximum flow velocity is reached one day after the initiation of breaching. It is stressed that, in other cases, this may be earlier or later, depending on the geometrical characteristics of the sand fill involved in the breaching event. Also, the volume of sand may be very different from the case studied. Bank failure events reported from estuarine channels that are probably caused by breaching may involve several million cubic metres of sand, and produce very thick massive sands (Van den Berg *et al.*, 2002). There is no reason why breaching events of similar, or even larger, magnitude would not occur in submarine canyons, or other steep submarine slope locations where sands accumulate. In view of this, breaching events of relatively long duration should be considered as a serious alternative explanation to the origin of deep-water massive sands that are generally attributed to abrupt mass failures (e.g. Stow & Johansson, 2000).

CONCLUSION

For a given shear stress or flow velocity, the maximum erosion rate of a sand bed is largest in the size range of medium to coarse sand. At larger sediment sizes, the erosion rate reduces, because of the increase in weight of the grains and, at smaller sizes, the erosion is retarded by negative pore pressures in the bed generated by a shear dilatancy effect. The maximum erosion velocity in fine sands is determined by the penetration velocity of water into the bed from the ambient fluid. The negative pore pressures in the bed impede the immediate collapse of very steep slopes in fine sands. Instead, such slopes may exist in channel banks or large bars for some time as gradually retrograding features, up to more than 5 m high, known as breaches. Breaching and the turbidity current generated by it should be

considered as a serious alternative to liquefaction as the mechanism behind large subaqueous slope failures in fine sand. Sand masses trapped in the nearshore heads of submarine canyons such as Scripps Submarine Canyon are susceptible to breaching. Computational results of turbidity current velocity near the canyon bed, obtained with a one-dimensional model in which breach growth is incorporated, show satisfactory agreement with quasi-steady flow conditions near the canyon bed measured during a flushing event. This supports the hypothesis that breaching and subsequent ignitive turbidity currents are the main mechanisms of sand removal from the canyon head. Flow evolution and flow duration during a breaching event depend on the geometry and volume of the sand fill. Large breaching events may last for more than a day and might be the origin of some deep-water massive sands.

ACKNOWLEDGEMENTS

Dr M. Felix, Dr G. de Cesare, and Dr L. C. van Rijn are gratefully acknowledged for their critical reviews.

NOTATION

A = coefficient (–);
c = volumetric sand concentration (dimensionless or volume percentage);
$\bar{c}$ = flow thickness averaged sand volumetric concentration (dimensionless or volume percentage);
D_* = dimensionless grain size (Bonnefile) parameter (–);
D_{15} = 15th percentile of the cumulative bed material grain-size distribution (m);
D_{50} = median grain size (m);
E = sediment pick-up rate perpendicular to the bed (kg s^{-1} m^{-2});
E_w = water entrainment rate (dimensionless);
H = thickness of upper layer (m);
f_0 = Darcy–Weisbach friction coefficient of sand bed (–);
f_i = friction coefficient in internal boundary layer (–);
Fr_i = internal Froude number (–);
g = gravity acceleration (m s^{-2});
h = flow thickness (m);
k_0 = permeability of the undisturbed sand bed (m s^{-1});
k_l = permeability of the loose sand bed (m s^{-1});
m = power in erosion function (–);
n = power in erosion function (–);
n_l = porosity of the loose sand bed (dimensionless or percentage of volume);
n_0 = actual porosity of the sand bed (dimensionless or percentage of volume);
q = specific discharge = $\bar{u}h$ (m^2 s^{-1})
S = sedimentation rate of the sand bed (kg s^{-1} m^2);
s = distance along sand slope (m);
u = flow velocity (m s^{-1});
$\bar{u}$ = flow velocity averaged over flow layer thickness (m s^{-1});
τ_0 = bed shear stress (Pa);
τ_i = shear stress in the internal boundary layer (Pa);
Ri = gradient Richardson number (–);
Ri^* = overall Richardson number (–);
W_0 = fall velocity of single sand particle in still water (m s^{-1});
x = horizontal distance (m);
z = distance to the bed (m);
α = local bed slope angle (°);
δ = thickness of intermediate layer between density flow and ambient fluid (m);
ε = relative density difference between the suspension flow sublayer and the ambient seawater upper layer (–);
Δ = relative density of particles (–);
Δn = porosity increase of the sand bed from undisturbed to loose conditions (–);
θ = Shields; or particle mobility parameter (–);
θ_{cr} = critical value of particle mobility (Shields' criterion; –);
ν = kinematic viscosity of the sea water (m^2 s^{-1});
v_e = sand bed erosion velocity perpendicular to bed (m s^{-1});
v_{ent} = water entrainment rate (m s^{-1});
v_s = Shields' velocity for sand grains (m s^{-1});
v_{sed} = sedimentation velocity (m s^{-1});
v_{wal} = wall velocity (m s^{-1});
Φ = dimensionless erosion rate (–);
ρ = density of sediment water mixture at height z above the bed (kg m^{-3});
ρ_w = density of sea water (kg m^{-3});
ρ_s = density of particles (kg m^{-3});
ρ_m = density of sand–water suspension (kg m^{-3});
φ = angle-of-repose of the sand (°).

REFERENCES

Ashida, K. and **Egashira, S.** (1975) Basic study on turbidite currents. *Proc. Jpn Soc. Civ. Eng.*, **237,** 37–50.
Breusers, H.N.C. (1974) Suction of sand. *Bull. Int. Soc. Eng. Geol.*, **10,** 65–66.

Chamberlain, T.K. (1960) *Mechanics of mass sediment transport in Scripps Submarine Canyon, California*. Unpubl. Thesis, University of California, Los Angeles, 200 pp.

Chamberlain, T.K. (1964) Mass transport of sediment in the heads of Scripps Submarine Canyon, California. In: *Papers in Marine Geology, Shepard Commemorative Volume* (Ed. R.L. Miller), pp. 42–64. Macmillan, New York.

Coleman, S.E., Andrews, D.P. and **Webby, M.G.** (2002) Overtopping breaching of noncohesive homogeneous embankments. *J. Hydraul. Eng.*, **128,** 829–838.

De Cesare, G., Schleiss, A. and **Hermann, F.** (2001) Impact of turbidity currents on reservoir sedimentation. *J. Hydraul. Eng.*, **127,** 6–16.

Dietz, R.S. and **Knebel, H.J.** (1971) Trou Sans Fond Submarine Canyon: Yvory Coast, Africa. *Deep-Sea Res.*, **18,** 441–447.

Dill, R.B. (1964a) *Contemporary submarine erosion in Scripps Submarine Canyon*. Thesis, University of California, San Diego, 299 pp.

Dill, R.B. (1964b) Sedimentation and erosion in Scripps Submarine Canyon head. In: *Papers in Marine Geology, Shepard Commemorative Volume* (Ed. R.L. Miller), pp. 23–41. Macmillan, New York.

Felix, M. (2001) A two-dimensional numerical model for a turbidity current. In: *Particulate Gravity Currents* (Eds W.D. McCaffrey, B.C. Kneller and J. Peakall), *IAS Spec. Publ.*, **31,** 71–81.

Fukushima, Y., Parker, G. and **Pantin, H.M.** (1985) Prediction of ignitive turbidity currents in Scripps Submarine Canyon. *Mar. Geol.*, **67,** 55–81.

Inman, D.L., Nordstrom, C.E. and **Flick, R.E.** (1976) Currents in submarine canyons: an air–sea–land interaction. *Annu. Rev. Fluid Mech.*, **8,** 275–310.

Kneller, B.C. and **Branney, J.** (1995) Sustained high-density turbidity currents and the deposition of thick massive sands. *Sedimentology*, **42,** 607–616.

Lofquist, K. (1960) Flow and stress near an interface between liquids. *Phys. Fluids*, **3,** 158–175.

Marshall, N.F. (1978) Large storm-induced sediment slump reopens an unknown Scripps Submarine Canyon tributary. In: *Sedimentation in Submarine Canyons, Fans and Trenches* (Eds D.J. Stanley and G. Kelling), pp. 73–84. Dowden, Hutchinson and Ross, Stroutsburg, USA.

Mastbergen, D.R. (1989) *Zand-Water Mengselstromingen; Wiskundig Model Terrasvormig Stort*. Report Z299. Delft Hydraulics, Delft.

Meijer, K.L. and **Van Os, A.G.** (1976) Pore pressure near moving underwater slope. *J. Geotech. Eng.*, **102,** 361–372.

Mulder, T., Syvitski, J.P.M. and **Skene, K.I.** (1998) Modeling of erosion and deposition by turbidity currents generated at river mouths. *J. Sed. Res.*, **68,** 124–137.

Parker, G. (1982) Conditions for the ignition of catastrophic erosive turbidity currents. *Mar. Geol.*, **46,** 307–327.

Parker, G. (1996) Some speculations on the relation between channel morphology and channel-scale flow structures. *Coherent Flow Structures in Open Channels* (Eds P.J. Ashworth, S.J. Bennett, J.L. Best and S.J. McLelland), pp. 423–458. Wiley, Chichester.

Parker, G., Fukushima, Y. and **Pantin, H.M.** (1986) Self-accelerating turbidity currents. *J. Fluid Mech.*, **171,** 145–181.

Parker, G., Garcia, M., Fukushima, Y. and **W.** (1987) Experiments on turbidity currents over an erodible bed. *J. Hydraul. Res.*, **25,** 123–147.

Piper, D.J.W. (1970) Transport and deposition of Holocene sediment on La Jolla Deep Sea Fan, California. *Mar. Geol.*, **8,** 211–227.

Shepard, F.P. (1951) Mass movements in submarine canyon heads. *Trans. Am. Geophys. Union*, **32,** 405–418.

Shepard, F.P. and **Buffington, E.C.** (1968) La Jolla submarine fan-valley. *Mar. Geol.*, **6,** 107–143.

Shepard, F.P. and **Dill, R.F.** (1966) *Submarine Canyons and Other Sea Valleys*. Rand McNally, Chicago, 381 pp.

Shepard, F.P. and **Marshall, N.F.** (1978) Currents in submarine canyons and other sea valleys. In: *Sedimentation in Submarine Canyons, Fans and Trenches* (Eds D.J. Stanley and G. Kelling), pp. 3–14. Dowden, Hutchinson and Ross, Stroutsburg, USA.

Stow, A.V. and **Johansson, M.** (2000) Deep-water massive sands: nature, origin and hydrocarbon implications. *Mar. Petrol. Geol.*, **17,** 145–174.

Thorpe, A.S. (1973) Turbulence in stably stratified flows; a review of laboratory experiments. *Bound. Lay. Meteorol.*, **5,** 95–119.

Turner, J.S. (1973) *Buoyancy Effects in Fluids*. Cambridge University Press, 367 pp.

Van den Berg, J.H., Van Gelder, A. and **Mastbergen, D.R.** (2002) The importance of breaching as a mechanism of subaqueous slope failure in fine sand. *Sedimentology*, **49,** 81–95.

Van Kesteren, W.G.M., Steeghs, H.J.M.G. and **Mastbergen, D.R.** (1992) Pore water behaviour in dredging processes. In: *Proceedings XIII World Dredging Conference* (Ed. V.L. Van Dam), pp. 598–615. Universal Publishing Corporation, Bombay.

Van Rhee, C. and **Bezuijen, A.** (1998) The breaching of sand investigated in large-scale model tests. *Proc. Int. Coastal Eng. Conf. Copenhagen*, **3,** 2509–2519.

Van Rijn, L.C. (1984a) Sediment pick-up functions. *J. Hydraul. Eng.*, **110,** 1495–1502.

Van Rijn, L.C. (1984b) Sediment transport, part III: bed forms and alluvial roughness. *J. Hydraul. Eng.*, **110,** 1733–1754.

Van Rijn, L.C. (1993) *Principles of Sediment Transport in Rivers, Estuaries and Coastal Seas*. Aqua Publications, Amsterdam.

Visser, P. (1998) *Breach growth in sand dikes*. PhD Thesis, Delft University of Technology, Delft.

Winterwerp, J.C., Bakker, W.T., Mastbergen, D.R. and **Van Rossum, H.** (1992) Hyperconcentrated sand-water mixture flows over erodible bed. *J. Hydraul. Eng.*, **118,** 1508–1525.

Manuscript received 11 April 2002;
revision accepted 5 December 2002.